

# A new data structure for efficient search on isovists

Florent Grélard<sup>1</sup>, Mehdi Ayadi<sup>1</sup>, Mihaela Scuturici<sup>1</sup>, and Serge Miguet<sup>1</sup>

<sup>1</sup>Université de Lyon, Lyon 2 LIRIS F-69676 Lyon, France  
 {florent.grelard, mehdi.ayadi, mihaela.scuturici,  
 serge.miguet}@univ-lyon2.fr

November 11, 2022

## Abstract

Spatial data structures allow to make efficient queries on Geographical Information Systems (GIS). Spatial queries involve the geometry of the data, such as points, lines, or polygons. For instance, a spatial query could poll for the nearest restaurants from a given location. Spatial queries can be solved exhaustively by going through the entire data, which is prohibitive as the number of data points increases. In this article, we are interested in making efficient queries on infinitely long geometrical shapes. For instance, angular sectors, defined as the intersection of two half-spaces, are infinitely long. However, regular spatial data structures are not adapted to these geometrical shapes. We propose a new method allowing to make efficient spatial queries on angular sectors (i.e. whether a point is inside an angular sector). It builds a R-tree from the dual space of angular sectors. An extensive evaluation shows our method is faster than using a regular R-tree.

**Keywords**— Spatial data structure, R-tree, isovist, duality, projective geometry

## 1 Introduction

The integration of the visible space from the point of view of pedestrians is an important step in urban planning Turner et al. (2001). The visible space can be extracted from a photographic investigation, which is a documentary practice led by professional photographers (e.g. (Lawson-Peebles, 1988)). In a city, photographic investigations result in a collection of photographs, from which hypotheses are made about the inhabitants' lifestyle, the architectural process, or how the visible space is perceived in the city. Usually, these hypotheses are based on the fact that a small number of photographs share certain traits, such as architectural features. The process of highlighting these traits is impeded as the number of photographs increases. One approach is to group photographs near a given location on a map based on the assumption that geographically close photographs share similarities. However, the content of geographically close photographs can be completely different, in particular in cities, where the landscape is rapidly changing. Another approach is to group photographs based on

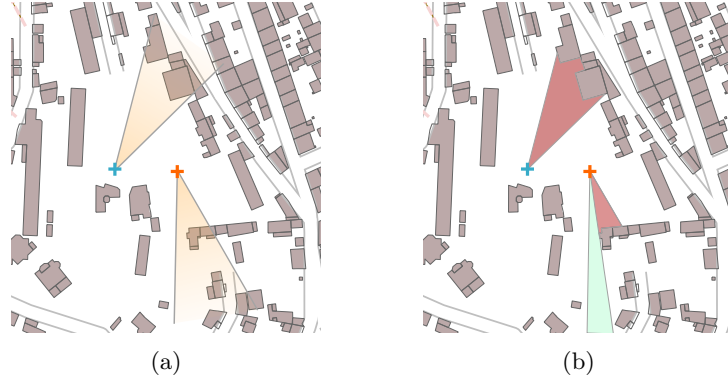


Figure 1: Typical spatial configuration in an urban environment with buildings (in gray) and visible space (in white). Two photographs (in blue and orange) with their associated (a) field of view (in pale orange) and (b) isovist (in red and green). (b) The isovist corresponds to the visible area from the point of view. The presence or absence of buildings defines areas with blocked visibility (in red) or free visibility (in green).

the points they visualize, that is to say their fields of view, as described by Ay et al. (2008) or Lu et al. (2014). This can also be achieved by searching the photographs based on their isovists.

The isovist is defined as the area of visible space from a given point of view (Benedikt, 1979). In an urban landscape, it allows to analyze the space layout by characterizing the impact of a building on the field of view of the photograph (see Fig. 1). It is computed from the position and direction of the photograph. For instance, the authors in Benedikt (1979) propose an algorithm to compute the isovist in 2D by joining the intersections between the building segments and rays drawn from the current position, in all directions. The drawback of such a method is that it is dependent on the number of rays: if it is too low, the resulting isovist is not accurate, and if it is too high, the computation time is prohibitive. The method introduced in Suleiman et al. (2013) maps building segments to the angle values they occupy in the field of view. The building segments are processed based on their distance: the closest segments to the photograph’s location are considered first. After they are mapped to an angle value, they are not considered further in the analysis.

Regardless of the method used for the isovist computation, the visibility is **blocked** when buildings obstruct the field of view (see Fig. 1b). In this case, the isovist is a polygon, that is to say, it has a bounded geometrical shape. On the contrary, when there is no building, the visibility is **free**, and the geometrical shape of the isovist is infinitely long. In this article, we focus on these infinitely long shapes in 2D.

In the following, the free-visibility areas in isovists are called angular sectors. Let  $l_1 : y = a_1x + b_1$  and  $l_2 : y = a_2x + b_2$  be non-parallel lines which intersect at  $a$ , with  $\tan^{-1}(a_1) < \tan^{-1}(a_2)$ . An angular sector of apex  $a$  is defined as the intersection between the half-spaces above  $l_1$  and below  $l_2$  (see Fig. 2). This point is called the apex  $a$  of the angular sector. An angular sector can be also represented thanks to three variables: the apex, the direction of the bisector, and the angle value at the apex.

The query “find all photographs which visualize a given point” can be achieved in logarithmic time with the R-tree (Guttman, 1984), for photographs with a bounded and small isovist. This is not the case for photographs with infinitely long geometrical shapes, i.e. angular sectors. In this article, we are interested in solving the following spatial query efficiently: “find all angular sectors which contain a given point”. This is

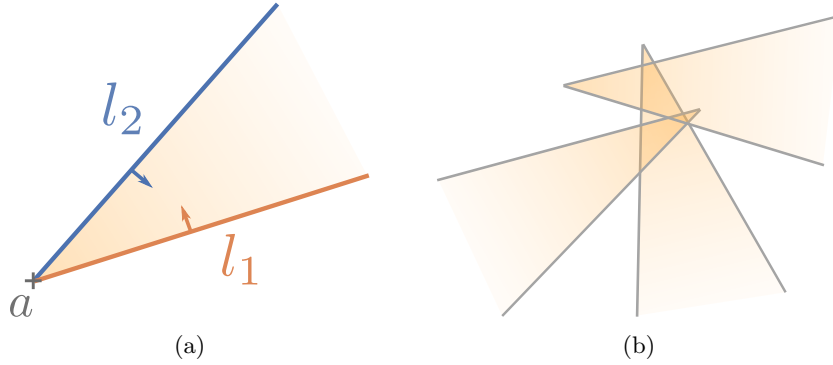


Figure 2: (a) Angular sector: intersection between two half-spaces: above the lower line  $l_1$  (in orange) and below the upper line  $l_2$  (in blue). The intersection between the two lines corresponds to the apex  $a$  of the sector. (b) Several angular sectors with different position and direction.

achieved by computing the intersection between the point and all the angular sectors. Such a query can be solved with an exhaustive search of all angular sectors, which is prohibitive as the number of photographs increases. Another approach would be to partition the space with evenly distributed angle intervals, from 0 to 360°, and to return the angular sectors present in the selected interval. However, this is not adapted to angular sectors with different positions because they can intersect despite having different angle values (see Fig. 2b). Moreover, logarithmic time could not be achieved, as it is not a recursive partition of the space.

In this article, we propose a new spatial data structure, called dual R-tree, to search efficiently through 2D angular sectors. The contributions of this paper are listed below.

- We review related methods from the literature in detail, and explain why they are not suited to the problem of searching efficiently through angular sectors.
- We describe two dual transforms which allow to convert infinitely long geometrical shapes to finite coordinates. These transforms are based on the existing duality between points and lines in the Euclidean space. This allows to convert a line to finite coordinates. We explain how the transforms are applicable to angular sectors.
- We introduce a new spatial data structure, called the dual R-tree. To the best of our knowledge, this is the first work on indexing angular sectors and infinitely-long geometrical shapes. The dual R-tree is an R-tree built on the dual coordinates of angular sectors. We also explain how to handle the limit-cases of the dual transforms in order to obtain a proper set of finite coordinates.
- Our method is evaluated on both synthetically generated data, and real-world data. The results show our method provides better optimization of the space inside of the tree, which translates in faster search times than the baseline methods. On the synthetic dataset, our method is at least five times faster than the baseline methods. These results are confirmed on the real-world dataset.

The article is organized as follows. In Section 2, we review the existing accelerating data structures. In Section 3, we recall the basics of dual transforms, which allow us to transform infinitely long geometrical shapes to bounded shapes. Section 4 describes our spatial data structure for angular sectors, based on dual transforms. In Section 5, we evaluate our method by comparison to a regular R-tree.

## 2 Related work

The authors in Ay et al. (2008) fully characterize a **field of view** of a photograph by four variables: the position (latitude and longitude values), the angle value, the direction and the visible distance (see Fig. 3). The latter variable corresponds to the restricting radius of the field of view and bounds the geometrical shape. This means the field of view is the bounded counterpart of angular sectors. Since, to the best of our knowledge, angular sectors have not been considered in the literature, this review is focused on existing methods on fields of views. Several accelerating spatial data structures were introduced in the literature for this type of data. More generally, the existing methods can be classified into two categories: the *space-driven* structures, and the *data-driven* structures.

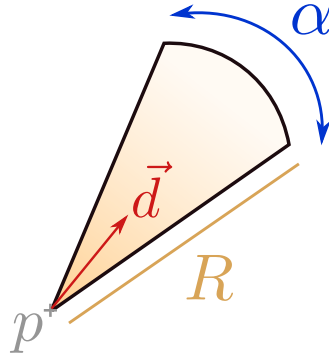


Figure 3: Field of view, defined by four variables (Ay et al., 2008): the position  $p$ , the angle value  $\alpha$ , the direction vector  $\vec{d}$  and the radius  $R$ .

The *space-driven* methods recursively partition the space, which allows to discard large portions of the space in the search procedure. They are comprised, among many others of the k-d tree (Bentley, 1975), the quadtree (Finkel and Bentley, 1974), Voronoi diagrams (Okabe et al., 2000), and the grid (Nievergelt et al., 1984). The grid partitions the space into regular rectangles, which is adapted to points, but not adapted to fields of view. The authors in Ma et al. (2013) propose a new grid structure for fields of view by defining three different hierarchical levels of space subdivision. The first level contains cells associated to the positions of the fields of view, the second level corresponds to their radius, and the third level is associated to their direction. During the search procedure, the positions and directions are processed separately, with predefined radius search range. For this reason, this structure is not adapted to geometrical shapes with infinite radius, such as angular sectors.

The *data-driven* structures revolve around the geometrical shape of the data. They are comprised, among many others of the R-tree (Guttman, 1984). The R-tree is a hierarchical data structure of rectangles, defined in Guttman (1984), and based on the B+-tree (Comer, 1979). The R-tree is a height-balanced tree, where the geometrical shapes are represented by their minimum bounding rectangles (see Fig. 5). These rectangles constitute the leaves in the R-tree (see Fig. 5b). The bounding rectangles are then grouped in larger, enclosing rectangles. A query which does not intersect an enclosing rectangle in the higher levels of the hierarchy does not intersect any of the enclosed rectangles. The branching factor determines the maximum number of children allowed at each node.

Several algorithms have been proposed to group rectangles so that a query yields as few false positive errors as possible. Usually, they involve optimizing various criteria, such as the coverage and overlap. These metrics quantify the amount of empty space

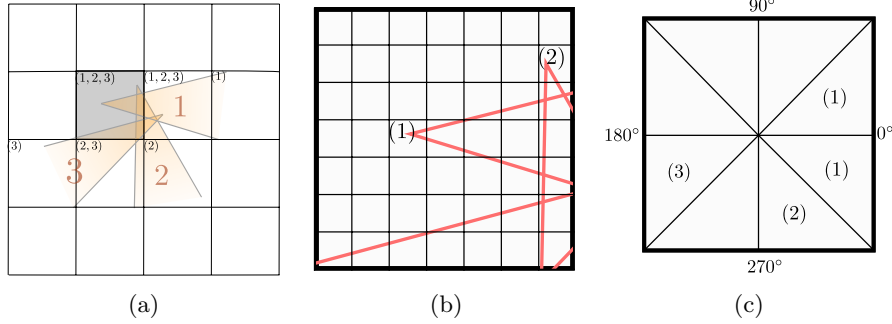


Figure 4: Example of a space-driven structure: the grid for three fields of view (denoted from 1 to 3, in orange), with three hierarchical levels Ma et al. (2013). The cell indices are noted in brackets inside the relevant cells. (a) First level, where cells indices correspond to the fields of view it contains. (b) Second level, close-up of the gray cell of Fig. (a). The cell indices correspond to the position of the field of view. Third level, where the grid is divided in sectors of regular intervals, where sector indices correspond to the direction of the field of view.

inside a node of the tree, that is to say the area of a minimum bounding rectangle which does not contain the enclosed geometrical data. The **coverage** is the ratio between the area covered by all enclosed rectangles and the area of the enclosing rectangle. The **overlap** is the ratio of the area covered by more than one rectangle with respect to the area of the enclosing rectangle. The R-tree allows to achieve  $\mathcal{O}(\log n)$  query time under the assumption that both the coverage and the overlap are minimized. When both the coverage approaches one and the overlap is low, the amount of empty space inside the enclosing rectangle is low. The authors in (Sellis et al., 1987) defined the R+-tree, which aims at optimizing both the coverage and the overlap, by splitting the minimum bounding rectangles and allowing the geometrical shapes to be added in various leaves.

In Ay et al. (2008), the authors use the minimum bounding rectangle of the field of view. The drawback of such a method is that the resulting rectangles in the hierarchy have a large amount of empty space. The authors in Lu et al. (2014), Lu et al. (2016), and Lu and Shahabi (2017) propose to minimize the amount of empty space by taking the direction of the field of view into account. The fields of views are enclosed in a minimum bounding field of view, which is a field of view enclosing its children. The search algorithm restricts the search to fields of view whose radius is less than a given distance. This structure is not adapted to angular sectors, since their radius is infinite.

More generally, the spatial data structures reviewed in this section are not adapted to infinitely long geometrical shapes, such as angular sectors. Indeed, they all consider bounded shapes, either during the insertion or the search procedure. In the next section, we propose a new method to make efficient queries on angular sectors.

### 3 Dual transforms

In the following, we review the affine and dual transforms, which convert infinitely long geometrical shapes to finite coordinates.

In the following, we are interested in **bi-angular sectors**, defined as the union of an angular sector, and its symmetric counterpart with respect to the apex (see Fig. 6a).

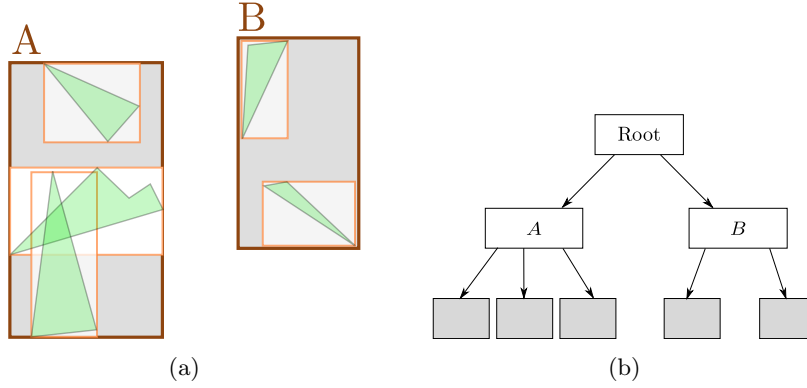


Figure 5: Indexing in the R-tree: (a) geometrical shapes (polygons from fields of view, in green) are represented by their minimum bounding rectangles (in orange). The empty space covers a large area for each polygon (in white). Rectangles are grouped in enclosing rectangles (A and B). (b) Resulting R-tree from the polygons in Fig. 5, where the minimum bounding rectangles correspond to the leaves of the tree (in gray).

### 3.1 Affine dual transform

The duality between points and lines stems from the observation that two points in the Euclidean space define a **single** line, and two lines intersect a **single** point (Poncelet, 1865). A line  $l : y = ax + b$  has two constants  $a$  and  $b$ , which define coordinates of a point  $p(a, b)$  in the parametric space of lines. Conversely, a point defines the coefficients of a line. The affine dual transform  $\delta_A$  maps a primal point to a dual line, and a primal line to a dual point. Let  $p = (x_p, y_p) \in \mathbb{R}^2$  be a point, and  $l$  be a non-vertical line. The affine dual transform is defined by:

$$p(x_p, y_p) \xrightarrow{\delta_A} p^* : y = x_p x - y_p \quad (1)$$

$$l : y = ax + b \xrightarrow{\delta_A} l^*(a, -b) \quad (2)$$

This transform is involutory, that is to say  $(p^*)^* = p$ . This transform has two additional interesting properties: incidence and order. Incidence means a point  $p$  is on a line  $l$  if and only if the point  $l^*$  is on the line  $p^*$ . Order means a point  $p$  is above the line  $l$  if and only if the point  $l^*$  is above the line  $p^*$ .

The dual bi-angular sector of lower and upper lines  $l_1$  and  $l_2$  is the segment joining the pair of coordinates  $l_1^*$  and  $l_2^*$  (see Fig. 6b). From the incidence property, it follows that the apex of the angular sector corresponds to the line passing through the segment  $l_1^* l_2^*$  in the dual space. From the order property, it follows that a point located inside an angular sector corresponds to a dual line which crosses the segment  $l_1^* l_2^*$ .

However, this transform cannot handle vertical lines, since their slope is not defined. Thus, two dual affine spaces are generally used: one for the lines with slope values less than one (*horizontal* lines), and another for the lines with slope values greater than one (*vertical* lines). Vertical lines can be expressed in the form of the equation  $l : x = my + n$ . Thus, the dual of a vertical line is the point  $l^*(m, -n)$ .

### 3.2 Polar dual transform

The polar dual transform  $\delta_P$ , also called  $\rho - \theta$ -parametrization, converts each line to a point and each point to a sinusoid (Radon, 1917). It can be applied to vertical lines,

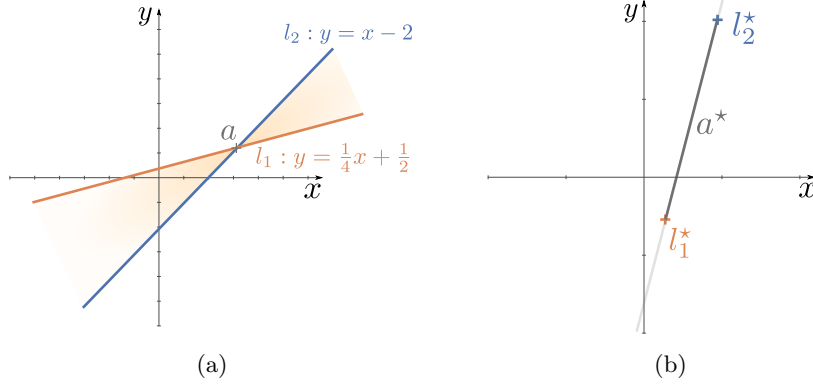


Figure 6: (a) Bi-angular sector of apex  $a$  defined by two lines: lower and upper lines ( $l_1$  and  $l_2$  in blue and orange, respectively), (b) Affine dual of the angular sector from Fig. 6a: segment joining the pair of dual coordinates ( $l_1^*$  and  $l_2^*$  in orange and blue). The apex  $a^*$  is a line (in light gray) joining these two coordinates.

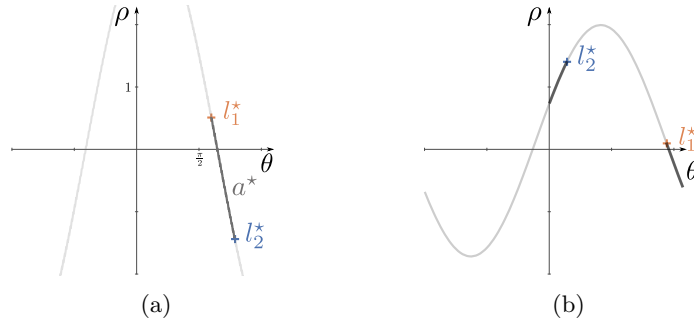


Figure 7: Polar dual of (a) the angular sector from Fig. 6a and (b) from an angular sector containing a vertical line. The dual angular sector is (a) the arc of the sinusoid  $a^*$ , or (b) the complementary of this arc on  $[0, \pi]$  for sectors containing vertical lines. The apex  $a^*$  is the sinusoid represented in light gray.

which makes it a strong candidate for angular sectors.

Let  $l: y = ax + b$  be a line, and  $H$  the orthogonal projection of the origin onto  $l$ , then  $\rho_H$  is the distance from the origin to  $H$ , and  $\theta_H$  is the angle between the  $x$ -axis and the line connecting the origin to  $H$ . The line  $l$  can be rewritten in the Hesse normal form as  $l: \rho_H = x \cos \theta_H + y \sin \theta_H$ . Then, the polar dual transform  $\delta_P$  is defined by:

$$p(x_p, y_p) \xrightarrow{\delta_P} p^*: \rho = x_p \cos \theta + y_p \sin \theta \quad (3)$$

$$l: \rho_H = x \cos \theta_H + y \sin \theta_H \xrightarrow{\delta_P} l^*(\theta_H, \rho_H) \quad (4)$$

A point in the polar dual space is defined by a pair of coordinates  $(\theta, \rho)$ , with  $\theta$  ranging from 0 to  $\pi$  and  $\rho \in \mathbb{R}$ , with  $\rho < 0$  if the ordinate of the point in the primal space is negative.

This transform verifies the incidence property: a point  $p$  is on a line  $l$  if the point  $l^*$  is on the sinusoid  $p^*$ . However, the order property does not hold for angular sectors

containing a vertical line. Indeed, the lower line is transformed into a dual point with a  $\theta$  value close to  $\pi$  and the upper line into a dual point with a  $\theta$  value close to 0.

This implies the following properties (see Fig. 7):

**Property 1** *For lines which **do not contain** a vertical line, a point  $p$  is located between two lines  $l_1$  and  $l_2$  if and only if the sinusoid  $p^*$  crosses the arc joining  $l_1^*$  and  $l_2^*$ .*

**Property 2** *For lines which **contain** a vertical line, a point  $p$  is located between two lines  $l_1$  and  $l_2$  if and only if the sinusoid  $p^*$  crosses the complementary of the arc joining  $l_1^*$  and  $l_2^*$ , on the interval  $[0, \pi]$ .*

The dual angular sector of lower and upper lines  $l_1$  and  $l_2$  is the arc of sinusoid joining  $l_1^*$  and  $l_2^*$  for angular sectors which do not contain a vertical line, and the complementary of this arc on  $[0, \pi]$  for sectors containing a vertical line. The dual apex  $a^*$  is the sinusoid passing through this arc.

## 4 Proposed method

Our method builds a spatial data structure from a dual transform, either the affine, or the polar dual. In the dual space, a bi-angular sector corresponds to a pair of finite coordinates. Thus, these dual coordinates can be inserted inside a hierarchical data structure with minimized overlap and coverage.

Our method is not dependent on the spatial data structure. We use the R-tree because it comes with various optimization strategies for split and loading, and is balanced, as opposed to the k-d tree. In the following, our method is referred to as the **dual R-tree**, and we describe its insertion and search procedures.

Regarding the insertion procedure, each dual angular sector is inserted as the minimum bounding rectangle of its pair of dual coordinates (see Fig. 8). These bounding rectangles correspond to the leaves inside the dual R-tree. The leaves also contain a reference to the primal angular sector in order to facilitate their retrieval. Strategies and optimizations from the R+-tree (see Section 2) are used to minimize the coverage and the overlap in the higher levels of the hierarchy.

Regarding the search algorithm, we are interested in three possible spatial queries: point, range and directional queries. A search by point returns all the angular sectors containing this point, a search by range returns the angular sectors intersecting a circular query range, and search by direction returns the angular sectors intersecting a line.

Regarding point queries, the primal query point is converted to its dual, that is to say a line for the affine dual transform, or an arc of a sinusoid for the polar dual transform. The primal point is inside an angular sector if the dual of the query point intersects the segment joining the dual coordinates. The nodes of the R-tree are traversed by a breadth-first search, starting from the root of the tree. If a node intersects a dual query point, its children are considered further in the search procedure, otherwise, its children are discarded. During the search procedure, an enclosing rectangle is discarded if it does not intersect the dual of the query point. This method might yield some false positives, in particular if the dual of the query point intersects the bounding rectangle but not the dual of the apex  $a^*$ . However, in our case, the angular sectors have a small angle (typically lower than  $10^\circ$ ), so the difference in  $\theta$ -coordinates for the pair of dual points is small, and the amount of empty space in the rectangle is negligible compared to the area of the enclosing rectangle. The assumptions we make on the angle distribution of our data is discussed further in Section 5.

A directional query is transformed into a single point in the dual space, so it can be processed similarly to point queries. A range query results in a collection of lines in



**Algorithm 1:** Building the dual R-tree.

**Data:**  $S$ : primal angular sectors,  $R$ : empty R-tree  
**Result:**  $R$ : Dual R-tree

```

1 forall  $s \in S$  do
2    $l_1 \leftarrow s.lowerLine$ ;
3    $l_2 \leftarrow s.upperLine$ ;
4    $l_1^* \leftarrow \delta(l_1)$ ;
5    $l_2^* \leftarrow \delta(l_2)$ ;
6    $r \leftarrow \text{MinimumBoundingRectangle}(l_1^*, l_2^*)$ ;
7    $R.insert(\{\text{rectangle} : r, \text{pointer} : s\})$ ;
8 end
9 return  $R$ 

```

the affine dual space, and a collection of sinusoids in the polar dual space. Processing this collection entirely does not result in an efficient search procedure. In the following, the spatial queries are restricted to points. The same methods are also applicable to directional queries.

The search procedure returns a list of bi-angular sectors. However, the initial query is to find **mono**-angular sectors (see Section 1). This means the resulting list must be trimmed of the irrelevant half of the sectors. Let  $n$  be the initial length of the list of sectors, and  $k$  the length of the list obtained after the search on the dual R-tree, this operation is achieved in  $\mathcal{O}(k)$  time, with  $k \ll n$ .

The dual R-tree can be built from either the affine, or the polar dual transforms. In the following, we describe the specificities pertaining to the type of duality, regarding the insertion and search procedures.

#### 4.1 Affine dual R-tree

The affine dual transform is not adapted to vertical lines, as described in Section 3.1. It is necessary to maintain two data structures: two R-trees  $R_H$  and  $R_V$  are built from the two affine dual transforms.  $R_H$  is associated with the transform  $T_H$  where the lines are expressed as  $y = ax + b$  (for *horizontal* lines), and  $R_V$  is associated with the transform  $T_V$  where the lines are expressed as  $x = my + n$  (for *vertical* lines). The latter expression effectively rotates the coordinate system ninety degrees clockwise. This means the initial vertical lines appear horizontal in this coordinate system. Two dual angular sectors  $A_H^*$  and  $A_V^*$  are obtained by the transforms  $T_H$  and  $T_V$ , respectively. In order to ensure the overlap is minimized, only the dual angular sector with the lowest distance between its pair of coordinates is kept, and its minimum bounding rectangle is added to the corresponding R-tree.

Both the R-trees  $R_H$  and  $R_V$  are polled during the search procedure. Let  $p = (x_p, y_p)$  be the input query point in the primal space, this point is converted to two dual lines  $p_H^* : y = x_p x - y_p$  and  $p_V^* : x = y_p y - x_p$  by  $T_H$  and  $T_V$  respectively. The tree  $R_H$  is traversed by a breadth-first search, and we check whether the rectangles intersect the line  $p_H^*$ . The same procedure is repeated between the rectangles of  $R_V$  and the line  $p_V^*$ .

#### 4.2 Polar dual R-tree

The polar dual transform can handle vertical lines, which means only one data structure needs to be maintained. For most angular sectors, the enclosing rectangle is the bounding box of the dual of the angular sector. However, two special cases need to be

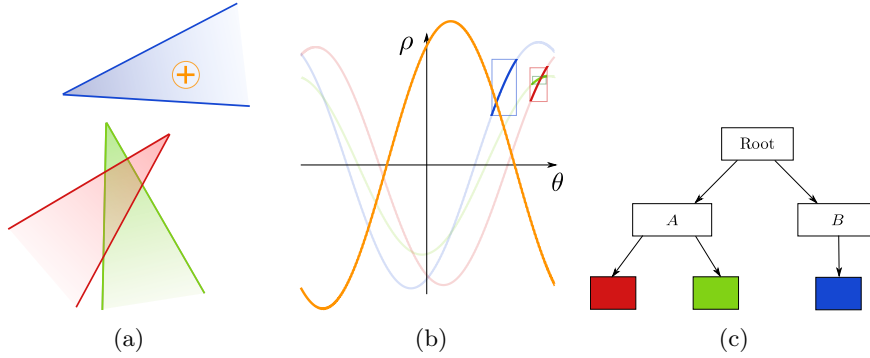


Figure 8: Overview of our method for the insertion and search of angular sectors inside the spatial data structure. (a) Primal angular sectors (in red, green and blue). We want to find all sectors containing the query point (in orange). The red and green angular sectors intersect. (b) Transformation of the primal angular sectors of Fig. (a) by the polar dual transform. The primal apices are transformed into sinusoids (in pale colors). The dual angular sectors correspond to arcs of sinusoids (in bright colors). The bounding rectangle of each arc of sinusoid form the leaves of our spatial data structure. The query point is transformed into a sinusoid (in orange) which intersects the rectangle of the blue dual angular sector. (c) Dual spatial data structure where each color corresponds to the respective bounding rectangle from Fig. (b).

considered. First, for an angular sector containing a vertical line, the dual transform does not preserve the order (see Section 3). In this case, two bounding rectangles are inserted inside the R-tree, for each primal lines delimiting the angular sector. The bounding rectangle for the lower line spans the range  $[\theta_{\text{lower}}, \pi]$ , and the bounding rectangle for the upper line spans the range  $[0, \theta_{\text{upper}}]$ . Secondly, in the case where the arc of the sinusoid joining two dual points reaches an extremum, the enclosing rectangle of the dual angular sector is not large enough to fully contain the arc of the sinusoid. In this case, the extremum is computed and the enclosing rectangle is extended in order to contain it (see Fig. 9).

Regarding the search procedure, the input query point  $p = (a, b)$  is transformed into a sinusoid in the dual space. The primal point is inside a given angular sector if the sinusoid intersects the bounding rectangle of the dual angular sector. In the following, we describe an efficient algorithm which allows to check whether a sinusoid intersects a rectangle.

Let  $A = \sqrt{a^2 + b^2}$  and  $\alpha = \tan^{-1}(\frac{b}{a})$ , the sinusoid  $\rho = a \cos \theta + b \sin \theta$  can be rewritten as :

$$\rho = A \cos(\theta - \alpha)$$

This form allows to compute the images and inverse images through the sinusoid for the lower and upper bounds of a given enclosing rectangle. If any of the images or inverse images are within the bounds of an enclosing rectangle, then the sinusoid intersects this rectangle (see Fig. 8b).

There are usually several inverse images through a given sinusoid. One inverse image of  $\rho$  is given by :

$$\theta(\rho) = \cos^{-1}(\frac{\rho}{A}) + \alpha$$

Since  $\alpha$  ranges from  $-\frac{\pi}{2}$  to  $\frac{\pi}{2}$ ,  $\theta(\rho)$  might not be in the range  $[0, \pi]$ . However, it is straightforward to show that the period of the query sinusoid is  $2\pi$ , so the other

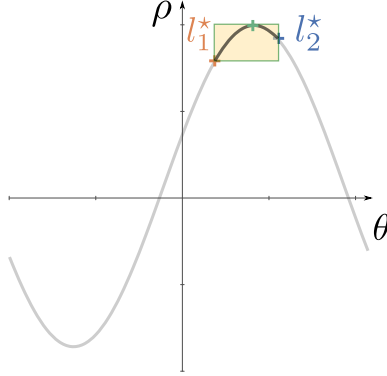


Figure 9: Corrected minimum bounding rectangle (in pale yellow) for a dual angular sector (coordinates in blue and orange) whose arc reaches a local extremum (in green).

considered inverse image is :

$$\theta(\rho) = \cos^{-1}\left(\frac{\rho}{A}\right) + \alpha + 2\pi$$

In total, two images and four inverse images are computed, for the lower and upper bounds of the rectangle. The computation of the intersection between a sinusoid and a rectangle is thus achieved in  $\mathcal{O}(1)$  time.

## 5 Experimental evaluation

In this section, we evaluate our dual spatial data structure. First, we explain the experimental datasets and methods used for the evaluation, and describe and analyze the results.

### 5.1 Experimental setting

Our data structure has been implemented using the RBush library<sup>1</sup>.

**Choice for the dual transform** In Section 4, the dual R-tree is built from either the affine or the polar transform. R-trees built from either transform yield a similar average search time regardless of the number of angular sectors (see Fig. 10). For example, for one million angular sectors, the average search time is 13 milliseconds (ms) for the R-tree built from the polar transform versus 10 ms for the affine transform. However, two data structures need to be maintained when the affine dual transform is used. The effective cost in memory might be prohibitive as the number of sectors increases. The polar dual transform only maintains one spatial data structure so, in the remainder of the evaluation, we choose this dual transform.

**Datasets** We used two types of datasets: synthetic data, and real data.

The synthetic data have been generated by fitting a model on the distribution of real data. The fields of view of 500 photographs, taken in an urban environment, were used to compute their isovists. Free visibility areas in the isovists constitute the angular sectors (see Section 1). The angle distribution for the 500 photographs is

<sup>1</sup><https://github.com/mourner/rbush>

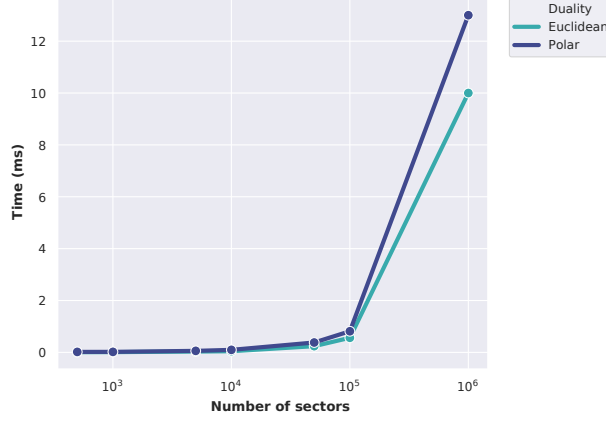


Figure 10: Average search time (in milliseconds, logarithmic scale) as a function of the number of sectors, for the affine or the polar transforms. They both display the same behavior, with minor differences in search time.

shown in Fig. 11. Synthetic angular sectors were generated with angle values chosen to fit this distribution.

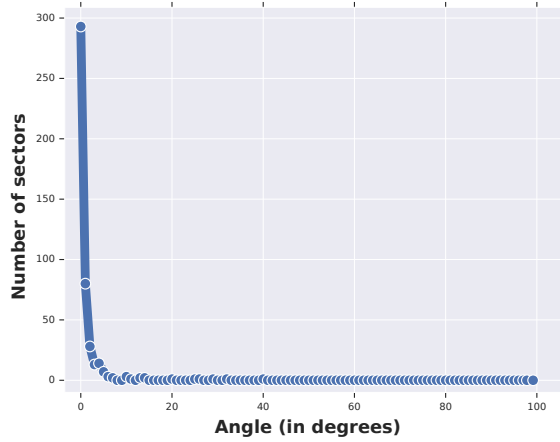


Figure 11: Angle distribution of angular sectors obtained from 500 photographs.

The real dataset was obtained from geo-tagged photographs from both Flickr<sup>2</sup> and the open building footprint dataset from the city of Chicago<sup>3</sup>. The photographs contain both position and direction information from which the isovists were extracted. The **full** dataset consists in the free visibility areas of the isovists (i.e. angular sectors). This dataset contains photographs located outside the building footprint area, in the country close to Chicago, typically. Thus, the associated angular sectors effectively correspond to the full field of view of the photograph. We generated an **urban**

<sup>2</sup><https://www.flickr.com/services/api/>

<sup>3</sup><https://data.cityofchicago.org/>

dataset by removing these angular sectors from the full dataset. From the  $9.0 \times 10^4$  photographs polled from Flickr, the full dataset contains about  $1.5 \times 10^5$  free visibility angular sectors, and the urban dataset about  $1.2 \times 10^5$  elements.

In the following evaluation, the angular sectors need to be bounded to be inserted inside the regular R-tree. They are represented as polygons with a size of  $10^8$  meters, which is deemed infinitely long at country scale.

**Metrics and baseline methods** We evaluate the search procedure on the dual R-tree, as the number of sectors increases. Its efficiency is assessed by several metrics: the initialization time (i.e. the time for the data structure to be fully built), the average search time, the length of the returned list (in number of elements), and the coverage and overlap measures inside the spatial data structure (see Section 2). The coverage and overlap measures allow to quantify the amount of empty space inside the R-tree, which is directly linked to the efficiency of the search procedure. Let  $r$  be a rectangle inside the R-tree,  $C$  the child rectangles  $r$  encloses,  $I_C = \{c_i \cap c_j, \forall (c_i, c_j) \in C \text{ s.t. } j > i\}$  the total intersection between child rectangles, and  $\text{Area}(s)$  the area of an arbitrary shape  $s$ .

The coverage for  $r$  is given by:

$$\text{coverage}(r) = \frac{\text{Area}(C)}{A(r)}$$

The overlap inside  $r$  is given by:

$$\text{overlap}(r) = \frac{\text{Area}(I_C)}{A(r)}$$

Joint values of one for the coverage and 0 for the overlap means there is no empty space inside a rectangle.

The point queries are made randomly in a region of 5x5 kilometers around the average position of the angular sectors. We compare our method to an **exhaustive search** (linear time) and to the search in a **regular R-tree** from the equivalent angular sectors. While the dual R-tree is built from bi-angular sectors, the search by the baseline methods is made on mono-angular sectors, as defined in Section 1. This allows to restrict the coverage and overlap for the regular R-tree, and is more in tune with the initial query. The branching factor for the R-tree is fixed at 7 throughout the experiments, as it showed a good compromise between number of access and size of the array resulting from the search procedure (results not shown).

## 5.2 Experimental results

### 5.2.1 Synthetic data

There are no major discrepancies in the initialization time between the dual R-tree and regular R-tree (about 100ms on average).

The profile for the average search time on the synthetic data is shown in Fig. 12. For one million angular sectors, it is 5 times lower than the search time in the regular R-tree, and 6.5 times lower than the search time for the exhaustive algorithm. However, the profile shows our method does not achieve logarithmic query time. Indeed, the search time is proportional to the number of sectors (see Fig. 12a). This is because angular sectors are infinitely long geometrical shapes, so they permanently fill a portion of the 2D space. For a large number  $n$  of angular sectors of angle  $\alpha$  (in degrees), the average number of sectors going through a random point is given by  $\frac{n \times \alpha}{360}$ . This means the query time is proportional to  $n$  and dependent on  $\alpha$ . However, from our distribution, most angular sectors have a very small angle: 65% of sectors have an angle lower than one degree (see Fig. 11) which makes our method faster than the baseline methods.

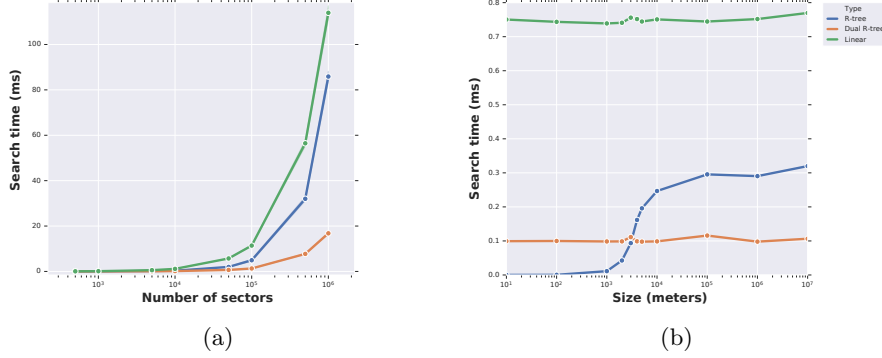


Figure 12: Average search time (in milliseconds) as a function of (a) the number of sectors (logarithmic scale) and (b) the size (in meters, logarithmic scale) for the R-tree built from our method (Dual R-tree, in orange), the R-tree built from primal angular sectors (regular R-tree, in blue) and the exhaustive search (Linear, in green). (a) For one million angular sectors, the search procedure from the dual R-tree is five times faster than the regular R-tree. (b) Our method is faster for angular sectors which length is greater than 400 meters.

We analyzed the search time as a function of the size (i.e. the radius) of the angular sectors (see Fig. 12b). Our method is not impacted by the size, but the regular R-tree is. When the size is small, the angular sectors are reduced to small polygons for which the regular R-tree is more efficient than our dual data structure. Our method is more efficient for angular sectors of length greater than 500 meters. Thus, it is suited not only for infinitely long geometrical shapes, but also for sufficiently large bounded ones.

The length of the returned array increases linearly with the number of sectors for both the R-tree and dual R-tree (see Fig. 13). The returned array is 6.5 times smaller with our method than with the regular R-tree. For one million sectors, the number of elements is about  $4 \times 10^4$  for our method, compared to  $2.6 \times 10^5$  for the regular R-tree. In order to remove the false positives inside the array, it is necessary to process the resulting arrays further. For the dual R-tree, this step is especially important in order to prune the irrelevant symmetric parts of the bi-angular sectors (see Section 3).

Results for the average coverage and overlap measures for all nodes in the tree are shown in Figure 14. The coverage values for the dual R-tree are closer to one than those of the regular R-tree. This is combined with low overlap values for the dual R-tree, which means there is less empty space inside the tree. It allows for faster elimination of negative results during the search procedure. This translates in an efficient data structure allowing to quickly search through angular sectors.

### 5.2.2 Real data

The results for the real dataset, for photographs from the city of Chicago is shown in Table 1.

Our method is more efficient for both datasets, compared to baseline methods. The average search time is lower, the coverage is close to one, and the overlap is lower than the regular R-tree. Nevertheless, the efficiency of the dual R-tree is not as obvious for the full dataset, as the search time is half of the search time on a regular R-tree. This dataset contains a large number of angular sectors with high angle values so it does not fulfill the hypotheses made on angle values, and is, as such, not well-suited to our method. The results are provided for the sake of completeness, and prove our

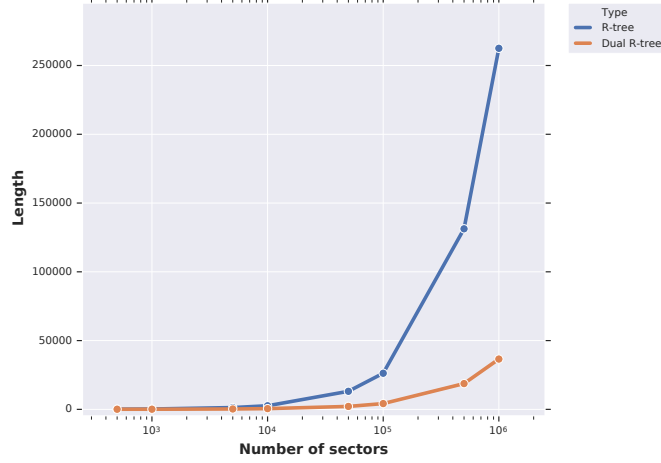


Figure 13: Length of the resulting array after the search, as a function of the number of sectors (logarithmic scale).

method is better suited for angular sectors with low angle values, typically found from photographs in a city, rather than in the country.

The results obtained on the urban dataset are in line with those obtained on the synthetic dataset. The average search time is four times lower than that of the regular R-tree, and the better values for the coverage and overlap mean there is less empty space inside the tree.

## 6 Conclusion

In this article, we have introduced a new method to search through angular sectors. The infinitely long angular sectors are converted to finite coordinates by dual transforms. Then, a spatial data structure is built from these coordinates. In Section 5, we explained why the search procedure cannot achieve  $\mathcal{O}(\log n)$  time. However, the results show our method provide faster results than existing spatial data structures when searching through a large number of angular sectors. Moreover, our method is not dependent on the size of the angular sectors, and is suited to sufficiently-large bounded polygons. It can be used to search efficiently through free-visibility areas of isovists in a city.

The amount of empty space inside the dual R-tree could be reduced by taking into account the shape of the dual angular sector. For instance, our method could be improved by transposing the OR-tree (see Section 2) to dual coordinates.

Our method is suited for 2D angular sectors. Recently, 3D city models have become more and more prominent, and 3D isovists can be extracted from them. We plan to extend our method to 3D, by transforming the 3D angular sectors with an adapted dual transform, such as the one from Borrmann et al. (2010).

## Acknowledgements

This work was part of the Optimum project (Observatoire photographique du territoire : images des mondes urbains en mutation) led by Danièle Méaux and with the fruitful

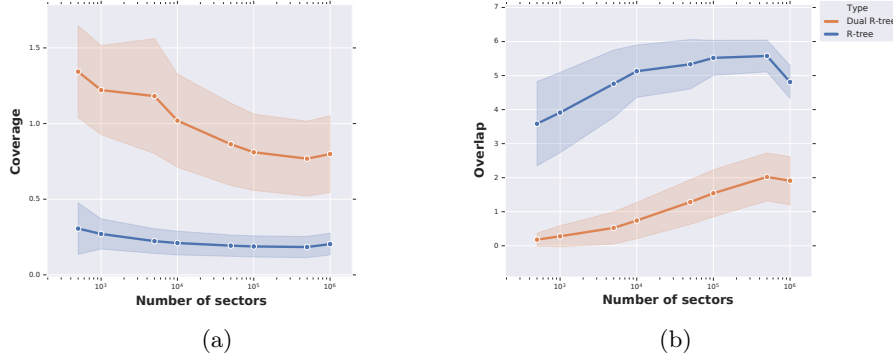


Figure 14: Average (a) coverage and (b) overlap measures as a function of the number of sectors (logarithmic scale), for the R-tree built from our method, with dual angular sectors (Dual R-tree, in orange), and the R-tree built from primal angular sectors (regular R-tree, in blue). (a) The dual R-tree has coverage values closer to one compared to the regular R-tree. (b) The overlap values for the dual R-tree are lower than those of the regular R-tree. For  $10^6$  sectors, there is a non-proportional increase in the number of available rectangles in the lower levels of the hierarchy. Thus, the overlap decreases for both trees.

participation of Guillaume Bonnel. This project was supported by the LABEX IMU (ANR-10-LABX-0088) of Université de Lyon, within the program “Investissements d’avenir” (ANR-11-IDEX-0007) operated by the French National Research Agency (ANR).

## References

- Ay, S. A., Zimmermann, R., and Kim, S. H. (2008). Viewable scene modeling for geospatial video search. In *Proceeding of the 16th ACM international conference on Multimedia - MM '08*. ACM Press.
- Benedikt, M. (1979). To take hold of space: Isovists and isovist fields. *Environment and Planning B: Planning and Design*, 6:47–65.
- Bentley, J. L. (1975). Multidimensional binary search trees used for associative searching. *Commun. ACM*, 18(9):509–517.
- Borrmann, D., Elseberg, J., Lingemann, K., and Nüchter, A. (2010). A data structure for the 3D Hough Transform for plane detection. *IFAC Proceedings Volumes*, 43(16):49 – 54. 7th IFAC Symposium on Intelligent Autonomous Vehicles.
- Comer, D. (1979). Ubiquitous B-Tree. *ACM Comput. Surv.*, 11(2):121–137.
- Finkel, R. A. and Bentley, J. L. (1974). Quad trees a data structure for retrieval on composite keys. *Acta Informatica*, 4(1):1–9.
- Guttman, A. (1984). R-trees: A dynamic index structure for spatial searching. *SIGMOD Rec.*, 14(2):47–57.
- Lawson-Peebles, R. (1988). John brinckerhoff jackson, discovering the vernacular landscape (new haven & london: Yale university press, 1984, £14.95) pp. 166. ISBN 0



Table 1: Results obtained by our method compared to the regular R-tree and an exhaustive search on angular sectors from photographs of Chicago (Flickr data), for the full dataset ( $1.5 \times 10^5$  angular sectors) and the urban dataset ( $1.2 \times 10^5$  angular sectors). Our method provides lower search times for both datasets, and better values for both the coverage and the overlap.

		Build time (ms)	Average search time (ms)	Coverage	Overlap
Full	Linear	N/A	9.41	N/A	N/A
	R-tree	175	6.20	0.26	8.79
	Dual R-tree	199	3.43	0.87	2.02
Urban	Linear	N/A	6.84	N/A	N/A
	R-tree	130	3.03	0.30	8.27
	Dual R-tree	165	0.776	1.08	1.59

300 03138 6. - richard p. horwitz, the strip: An american place. photographs by karin e. becker. (lincoln & london: University of nebraska press, 1985, \$14.95). pp. 188. ISBN 8032 7228 6. *Journal of American Studies*, 22(1):149–151.

Lu, Y. and Shahabi, C. (2017). Efficient indexing and querying of geo-tagged aerial videos. In *Proceedings of the 25th ACM SIGSPATIAL International Conference on Advances in Geographic Information Systems - SIGSPATIAL'17*. ACM Press.

Lu, Y., Shahabi, C., and Kim, S. H. (2014). An efficient index structure for large-scale geo-tagged video databases. In *Proceedings of the 22nd ACM SIGSPATIAL International Conference on Advances in Geographic Information Systems - SIGSPATIAL '14*. ACM Press.

Lu, Y., Shahabi, C., and Kim, S. H. (2016). Efficient indexing and retrieval of large-scale geo-tagged video databases. *GeoInformatica*, 20(4):829–857.

Ma, H., Ay, S. A., Zimmermann, R., and Kim, S. H. (2013). Large-scale geo-tagged video indexing and queries. *GeoInformatica*, 18(4):671–697.

Nievergelt, J., Hinterberger, H., and Sevcik, K. C. (1984). The grid file: An adaptable, symmetric multikey file structure. *ACM Transactions on Database Systems*, 9(1):38–71.

Okabe, A., Boots, B., Sugihara, K., Chiu, S. N., and Kendall, D. G., editors (2000). *Spatial Tessellations*. John Wiley & Sons, Inc.

Poncelet, J. (1865). *Traité des propriétés projectives des figures: ouvrage utile à ceux qui s'occupent des applications de la géométrie descriptive et d'opérations géométriques sur le terrain*. Number 1. Gauthier-Villars.

Radon, J. (1917). On the determination of functions from their integral values along certain manifolds. *IEEE Transactions on Medical Imaging*, 5(4):170–176.

Sellis, T. K., Roussopoulos, N., and Faloutsos, C. (1987). The R+-Tree: A dynamic index for multi-dimensional objects. In *Proceedings of the 13th International Conference on Very Large Data Bases, VLDB '87*, pages 507–518, San Francisco, CA, USA. Morgan Kaufmann Publishers Inc.

Suleiman, W., Joliveau, T., and Favier, E. (2013). *A New Algorithm for 3D Isovists*, pages 157–173. Springer Berlin Heidelberg, Berlin, Heidelberg.

Turner, A., Doxa, M., O'Sullivan, D., and Penn, A. (2001). From isovists to visibility graphs: A methodology for the analysis of architectural space. *Environment and Planning B: Planning and Design*, 28(1):103–121.